



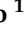




Article

An Increase in the Energy Efficiency of a New Design of Pumps for Nuclear Power Plants

Ivan Pavlenko ^{1,2,*} , Olaf Cizsak ³ , Vladyslav Kondus ^{1,4} , Oleksandr Ratushnyi ¹ , Oleksandr Ivchenko ¹ , Eduard Kolisnichenko ¹, Oleksandr Kulikov ¹  and Vitalii Ivanov ^{1,2} 

¹ Faculty of Technical Systems and Energy Efficient Technologies, Sumy State University, 2, Rymaskogo-Korsakova St., 40007 Sumy, Ukraine; ivanov@tmvi.sumdu.edu.ua (V.I.)

² Faculty of Manufacturing Technologies with a Seat in Prešov, Technical University of Košice, 1, Bayerova St., 080 01 Prešov, Slovakia

³ Faculty of Mechanical Engineering, Poznań University of Technology, 5, Marii Skłodowskiej-Curie Sq., 60-965 Poznań, Poland; olaf.cizsak@put.poznan.pl

⁴ Sumy Machine-Building Cluster of Energy Equipment, Sumy State University, 2, Rymaskogo-Korsakova St., 40007 Sumy, Ukraine

* Correspondence: i.pavlenko@cm.sumdu.edu.ua

Abstract: The reliability of pumping units at nuclear power plants (NPPs) is critical in terms of their energy efficiency and safety. Remarkably, WWER-1000 reactors at Ukrainian NPPs are equipped with outdated pumping units that have already served their full-service life. This fact leads to an urgent need to develop a new, more efficient pump. In the article, a promising pump, ACNA 600-35, was developed. It was designed to increase the energy efficiency of pumps TX 800/70/8-K-2E, applied at the holding pool and the industrial circuit of the nuclear reactor. Since these pumps should be imported from the monopoly suppliers, this affects both the energy efficiency of pumping equipment and the energy independence of Eastern Europe. The proposed pump ACNA 600-35 is characterized by an increased efficiency of up to 0.12–0.13 compared with the TX 800/70/8-K-2E pump. In general, the life cycle cost of the proposed pump is 15–20% lower than for the analog TX 800/70/8-K-2E. The design of the developed pump ACNA 600-35 and the related pumping unit based on its production at industrial facilities allows for further development of the industrial and fuel-energy complex, increasing the state's energy independence and employment. According to expert estimates, the average economic effect from supplying the developed pump can reach 10 mln USD/year.

Keywords: energy efficiency; centrifugal pump; power consumption; process innovation; energy independence



Citation: Pavlenko, I.; Cizsak, O.; Kondus, V.; Ratushnyi, O.; Ivchenko, O.; Kolisnichenko, E.; Kulikov, O.; Ivanov, V. An Increase in the Energy Efficiency of a New Design of Pumps for Nuclear Power Plants. *Energies* **2023**, *16*, 2929. <https://doi.org/10.3390/en16062929>

Academic Editor: Alessia Arteconi

Received: 25 February 2023

Revised: 18 March 2023

Accepted: 20 March 2023

Published: 22 March 2023



Copyright: © 2023 by the authors. Licensee MDPI, Basel, Switzerland. This article is an open access article distributed under the terms and conditions of the Creative Commons Attribution (CC BY) license (<https://creativecommons.org/licenses/by/4.0/>).

1. Introduction

Pumping units of nuclear power plants (NPPs) are essential for such facilities' reliability, safety, and energy efficiency [1–3].

Given the place of installation, the main requirement for pumping units is the reliability of their operation. Currently, the WWER-1000 [4] reactors at NPPs are equipped with outdated pumping equipment, which have served their entire operational life, leading to an urgent need to develop a new, more efficient pump.

Presently, there is no production of pumps for the holding pool and the industrial circuit of the nuclear reactor, which significantly reduces the degree of energy security [5] because of the existing geopolitical challenges. For the specified needs, Ukrainian NPPs use TX 800/70/8-K-2E pumps. These pumps were developed as pumps for general industrial purposes and they should be imported from the monopoly producers. Thus, the failure of these pumps can significantly affect the supply of electricity to end consumers and the nuclear safety of Eastern Europe [6,7].

It is also essential that these pumps were developed in the middle of the 20th century. Therefore, now, they can be outdated [8] due to repair costs and low energy efficiency

indicators. Particularly, their energy efficiency does not exceed 63% [9]. This indicates a low technical level, requiring immediate improvement [10,11].

Introducing improved pumping units for the specified needs will increase the units' reliability and energy efficiency, solve the import substitution issue, and increase the energy efficiency of pumps TX 800/70/8-K-2E with modern pumping units at operating NPPs. Simultaneously, there is a need to increase the energy efficiency of 26 pumping units at existing NPPs and to equip new units of NPPs under construction with them (in particular, units 3 and 4 of the Khmelnytskyi NPP require the introduction of four pumping units to meet the above needs).

The following state-of-the-art, energy-efficient pumping equipment highlights the scientific and practical significance of the proposed research. Particularly, Capurso et al. [12] designed and performed a CFD performance analysis of a novel impeller for centrifugal pumps for NPPs. The obtained results demonstrated an efficiency improvement of 1–2% compared with conventional designs.

Fan et al. [13] studied the transient flow characteristics of centrifugal pumps for variable operating conditions at 1000 MW NPPs. As a result, it was proved that the hydraulic performance of the pump is influenced both by the fluid acceleration and instantaneous evolutions of the vortex structure during the transient process. Additionally, Zhou and Wang [14] studied the effects of blade stacking lean angle on 1400 MW canned nuclear coolant pump hydraulic performance.

Research on flow characteristics in a main nuclear power plant pump with an eccentric impeller was carried out by Ran et al. [15]. It was proven that impeller eccentricity leads to an increase in the amplitudes of forced oscillations. Additionally, Yu et al. [16] experimentally studied the effect of non-uniform flow on the vibration characteristics of the reactor coolant pump.

Qian et al. [17] proposed a two-stage centrifugal pump at NPPs. A new design allowed for an even-distributed pressure field and a fairly low turbulent kinetic energy field. Additionally, Liu et al. [18] proposed a fault recognition model for NPP's water pumps based on a frequency-domain data attention mechanism. Finally, Jiao et al. [19] simulated the idling of nuclear power coolant pumps considering the kinetic energy of the flow.

After considering the above-mentioned state-of-the-art developments, the following research aim and objectives have been formulated. Particularly, the main aim of the research is to ensure the reliability and energy efficiency of the functional elements of the cooling systems of the holding pool and the industrial circuit of the nuclear reactor WWER-1000 of NPPs.

To fulfill this goal, the following objectives should be reached. Firstly, the design scheme of the pump and construction of the elements of its flowing part should be developed. Secondly, numerical simulation of hydrodynamic processes in the elements of the developed pump's flowing part should be carried out in order to ensure a high level of energy efficiency and obtain the resulting energy characteristics of the pump. Finally, evaluation of the strength and vibration analyses of the pump's functional elements should be performed to prove a sufficient vibration reliability.

2. Materials and Methods

At the empirical stage of scientific research, the methods consisted of conducting physical experiments (experimental hydromechanics, direct observation, etc., with further processing using the Python programming language), numerical simulation (finite element analysis (FEA), and methods of computational fluid dynamics (CFD) in ANSYS CFX 19.0 software with further processing in the computer system algebra PTC MathCAD 15.0. The flowchart of the research methodology is presented in Figure 1.

The theoretical developments were verified using simulation modeling. The models are based on the actual designs of pumping equipment. It also includes a comparison of the obtained results for pressure head, vibration modes, and reliability of the designed pumping equipment with the passport data of the pumping equipment operated at the NPPs.

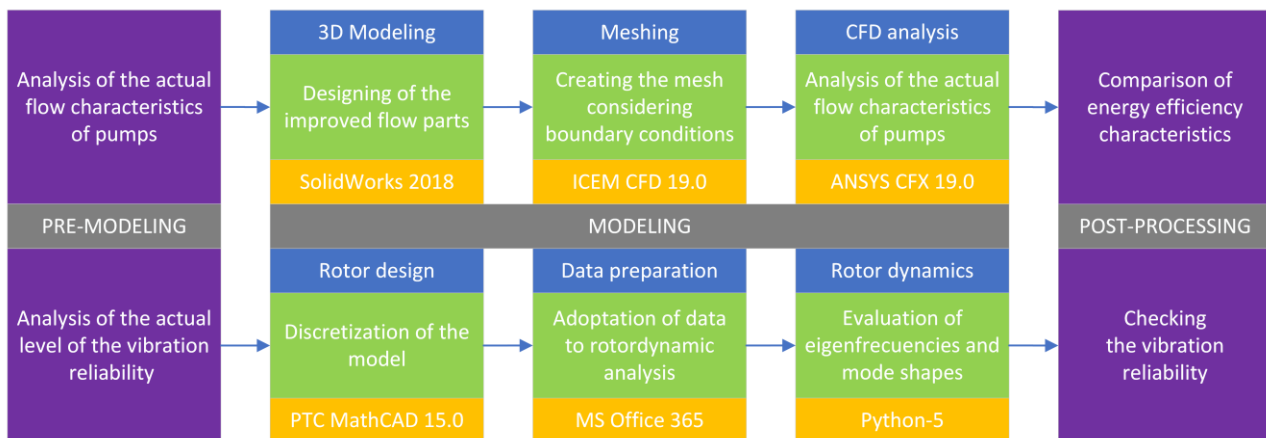


Figure 1. Flowchart of the research methodology.

The developed pump is marked as ACNA 600-35, where ACNA means a centrifugal pump unit, 600 m³/h is the flow rate, and 35 m is the pressure head.

To realize numerical simulations, ANSYS CFX 19.0 software has been used. The ICEM CFD 19.0 program package has been used to generate grids. The design of solid-state models of the calculation domains (stator and rotor) has been performed using SolidWorks 2018 software. This software is based on the numerical solution method of the fundamental laws of hydromechanics.

ANSYS CFX 19.0 has been repeatedly tested when solving similar problems in pump design. In all cases, the discrepancy between numerical and physical modeling results did not exceed 5% [20–23]. Given this, it can be argued that this software is suitable for solving the research problem.

Modeling of turbulent fluid flow was performed using Reynolds equations [24] ($i, j = 1-3$):

$$\frac{\partial}{\partial t}(\rho U_i) + \frac{\partial}{\partial x_i}(\rho U_i U_j) = -\frac{\partial p}{\partial x_j} + \frac{\partial}{\partial x_i} \left[\mu \left(\frac{\partial U_i}{\partial x_j} + \frac{\partial U_j}{\partial x_i} \right) \right] + f_i, \quad (1)$$

$$\frac{\partial p}{\partial t} + \frac{\partial}{\partial x_i}(\rho U_j) = 0, \quad (2)$$

where x_i, x_j —coordinate axes; U_i, U_j —velocity components; p —pressure; t —time; f_i — i -th mass force.

The term f_i in Equation (1) expresses the interaction of Coriolis and centrifugal forces in the relative reference frame, in which the operating process in dynamic hydraulic machines is considered:

$$\vec{f}_i = -\rho \left[2\vec{\omega} \times \vec{u} + \vec{\omega} \times (\vec{\omega} \times \vec{r}) \right], \quad (3)$$

where $\vec{\omega}$ —the angular velocity vector, \vec{r} —the radius vector.

While modeling turbulent flows according to the Navier–Stokes equations, the instantaneous velocity is replaced by the sum of the Reynolds averaged velocity and the pulsating velocity component. As a result, dependence (1) takes the following form:

$$\frac{\partial}{\partial t}(\rho \bar{U}_i) + \frac{\partial}{\partial x_i}(\rho \bar{U}_i \bar{U}_j) + \frac{\partial}{\partial x_j}(\rho \bar{U}_i' \bar{U}_j') = -\frac{\partial p}{\partial x_j} + \frac{\partial}{\partial x_i} \left[\mu \left(\frac{\partial \bar{U}_i}{\partial x_j} + \frac{\partial \bar{U}_j}{\partial x_i} \right) \right] + f_i, \quad (4)$$

where \bar{U}_i, \bar{U}_j —time-averaged velocity values; \bar{U}_i', \bar{U}_j' —pulsating components of velocities.

According to the ACNA 600-35 pump's developed design scheme, 3D models of the elements of its flowing part were designed using SolidWorks 2018 SP 5.0 software.

For the numerical research, unstructured meshes (Figure 2) generating the environment in the flowing part of the pump were constructed using the ICEM CFD mesh generator.

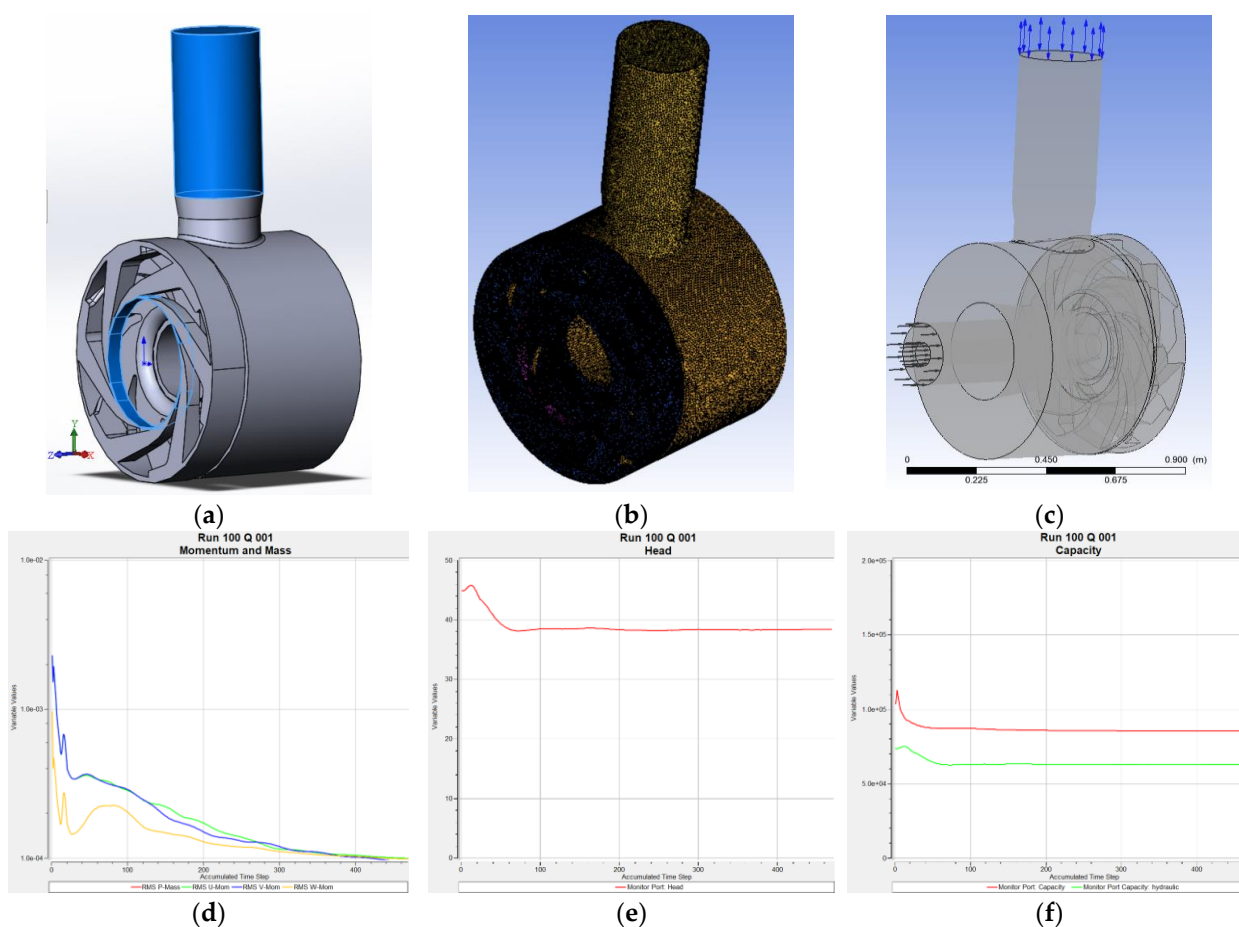


Figure 2. Preparation stages for the numerical simulations: (a) 3D model of the environment at the flowing part of the developed pump ACNA 600-35; (b) calculation mesh; (c) setting of interfaces during the numerical study; (d) mass and moments convergence parameters; (e) pressure convergence parameters; (f) convergence of output power and power consumption.

Eight prismatic cells were created to describe the boundary layer near solid walls. A preliminary study of grid independence was conducted. After generating the mesh, the output data was specified in the pre-processor. As a boundary condition, the mass flow was set at the inlet to the calculation area and static pressure at the outlet of it. For all solid bodies, the condition that the velocity on the surface is zero was given. The roughness of the walls was taken according to the working drawings of the parts of the pump's flowing part.

The parameter y^+ in the pump flowing part is mainly from 48 to 60. The most significant value of the parameter y^+ is 89. The value of the variable y , which characterizes the thickening of the grid near the walls, was within $20 < y^+ < 100$, corresponding to the recommendations given in the user manual [25].

The calculation domain consists of two parts: rotor and stator. The rotor part includes the impeller and the inlet device, and the stator part is the outlet device. The inlet device is part of the rotor grid, but its walls are stators.

The stator and rotor elements' calculated grids were unstructured using tetrahedral elements. The total number of cells of the rotor's elements was 2.136×10^6 cells, and the total number of the stator's elements was 2.836×10^6 . The smooth elements' global quality of the rotor elements was not lower than 0.296 and the rotor elements were not lower than 0.295. A prismatic wall grid consisting of 7 layers was built for both elements of the calculation area (rotor and stator) for qualitative modeling of the wall layer. Prismatic grid parameters are as follows: growth law—exponential; initial high—0.05 mm; height ratio—1.8; the total number of layers—7; the total height—3.764.

The calculation model specifies the parameters of the inlet, outlet, roughness of walls, and interfaces (Figure 2c). Next, numerical research was carried out with the achievement of convergence of parameters for mass and moments (Figure 2d), parameters for pressure (Figure 2e), and achievement of convergence of parameters for output power and power consumption (Figure 2f).

In order to calculate the strength and vibration resistance of the rotor of the centrifugal pump ACNA 600-35 using FEA, a modal analysis of the calculation scheme of the shaft was carried out according to the calculation scheme shown in Figure 3.

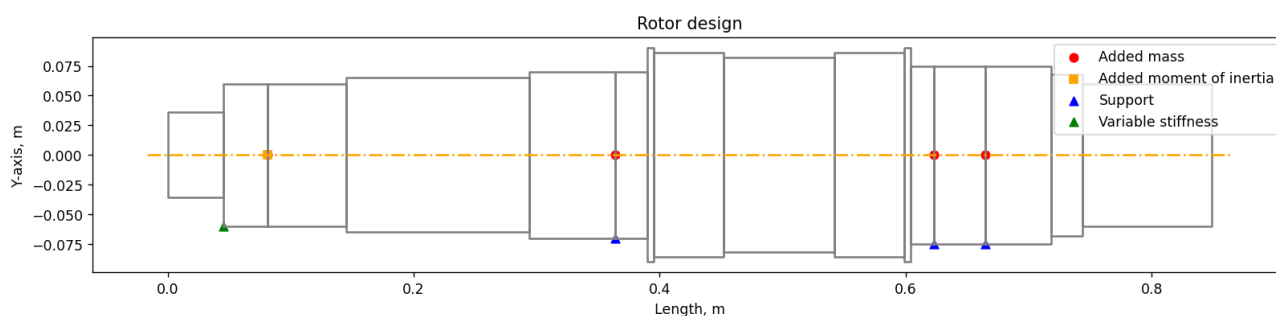


Figure 3. Calculation scheme of the finite element model.

The shaft was modeled by a three-dimensional beam element using the author's improved computer program "Critical frequencies of the rotor", realized by Python programming language, for modeling linear beam structures with an average length ratio to thickness, built on Timoshenko's beam model, considering shear deformations. The cross-section of each section was a circle with a diameter corresponding to the calculation scheme.

The pump in the pumping unit is centrifugal, horizontal, cantilever, and single-stage. It is designed for pumping chemically active and neutral liquids and suspensions with a temperature from $-40\text{ }^{\circ}\text{C}$ to $+120\text{ }^{\circ}\text{C}$, a density of no more than 1850 kg/m^3 , a viscosity of up to $30 \times 10^{-6}\text{ m}^2/\text{s}$, and containing solid inclusions no larger than 1 mm in size [26]. The volume concentration of inclusions should not exceed 15% with a size of no more than 5 mm and volume concentration of no more than 1% (Table 1).

Table 1. Operating parameters of the developed pump ACNA 600-35.

Characteristic	Indicator Value
Flow rate, m^3/h	600
Pressure head, m	35
Rotation speed, rpm	1485
Power, kW	
-pump	71.9 *
-pumping unit	75.6 *
Maximum power, kW	
-pump	86.3 *
-pumping unit	90.7 *
The maximum pressure at the pump outlet, MPa	1.17 *

* The value is given at a density of $\rho = 1005\text{ kg/m}^3$.

The shaft material is alloy steel AISI 420 with the following characteristics: Young's modulus $E = 1.97 \times 10^{11}\text{ Pa}$; Poisson's ratio $\mu = 0.3$; density $\rho = 7750\text{ kg/m}^3$.

To evaluate eigenfrequencies and the corresponding mode shapes, the Block Lanczos block method was used. The method of sparse matrices has been applied to solve systems of linear equations.

3. Results

3.1. Numerical Simulation of Hydrodynamic Processes in a Flowing Part

The calculation results analysis was carried out in ANSYS CFX-Post 19.0 software for post-processing. The characteristics of the pump's flowing part (Figure 4) were made to study the qualitative features of fluid movement through the pump and to make corrections to the structural elements.

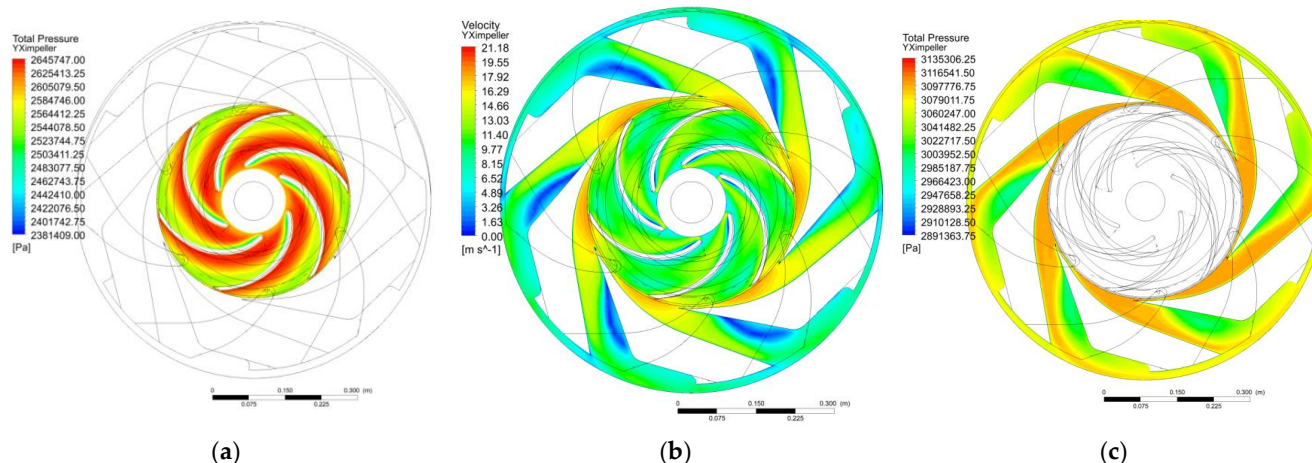


Figure 4. Characteristics of the pump flowing part: (a) pressure distribution in the intervane channels of the impeller; (b) a qualitative picture of the relative velocity distribution in the diffuser channel of the outlet device; (c) a qualitative picture of the pressure distribution in the diffuser channel of the outlet device.

Analysis of the qualitative picture of the distribution of relative speed in impeller intervane channels proves the high quality of the design of its flowing part.

The qualitative picture of the flow in the meridional section of the impeller proves the correctness of the installation angles of the main and cover discs. The existing zones of slightly reduced (blue color) and increased (red color) relative velocity are insignificant and are explained by the turning of the flow. At the same time, such zones are not predominant. Therefore, the meridional section of the impeller is made with high hydraulic qualities.

The distribution of pressure in the impeller intervane channels [27] proves the correct selection of the number of blades (Figure 4a). Zones with a slightly higher pressure value (red color) correspond with a position near the working side of the impeller blade, while zones with a lower pressure value (yellow color) correspond with a position near the back side of the blade. In general, the pressure drop in the impeller intervane channels does not exceed 100 kPa (or 3.8%), indicating that the impeller's flow part is correctly designed considering its number of blades.

The distribution of relative velocity in the diffuser channels of the pump outlet device (Figure 4b) indicates sufficient flow quality on the guide vanes device. The available zones of reduced pressure (blue color) are explained by a complex of factors, among which should be attributed: to the rotation of the flow during the transition from the diffuser channel to the transfer channel of the guide vanes device, the diffusive nature of flow movement in the diffuser channels of the outlet device, and the need to ensure the smallest possible radial dimensions of the pump for reduction of its mass and dimensional characteristics.

Similar conclusions can be made from the qualitative picture of pressure distribution in the diffuser channel of the outlet device (Figure 4c).

The results of CFD modeling in the transfer and outlet channels of the outlet device are presented in Figure 5.

Similar conclusions following can be made from the qualitative picture of pressure distribution in the transfer and outlet channels of the guide vanes (Figure 5a) since there are no clearly defined significant zones of reduced (blue color) or increased (red color) pressure.

The distribution of relative velocity in the annular chamber and the pressure nozzle of the pump (Figure 5b) is uniform, which confirms the presence of minimal hydraulic losses in these pump channels because there are no significant zones of vortex formation (blue color—zones of reduced speed, red—high-speed zone).

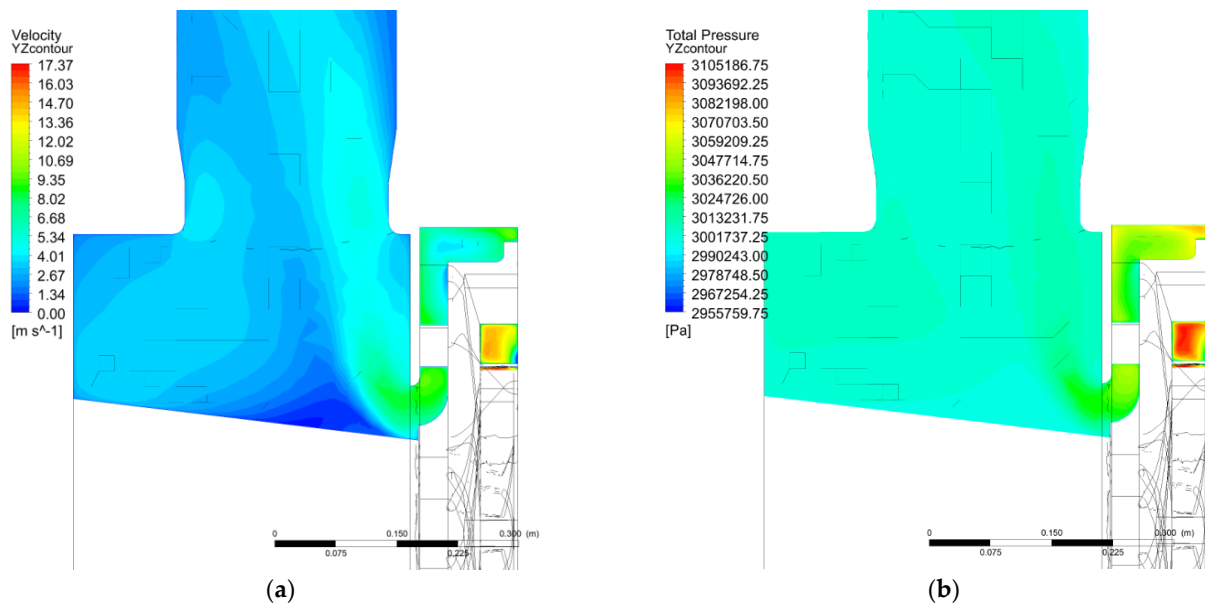


Figure 5. Results of the transfer and outlet channels of the outlet device: (a) a qualitative picture of the relative velocity distribution; (b) a qualitative picture of pressure distribution.

A qualitative picture of the distribution is presented in Figure 6.

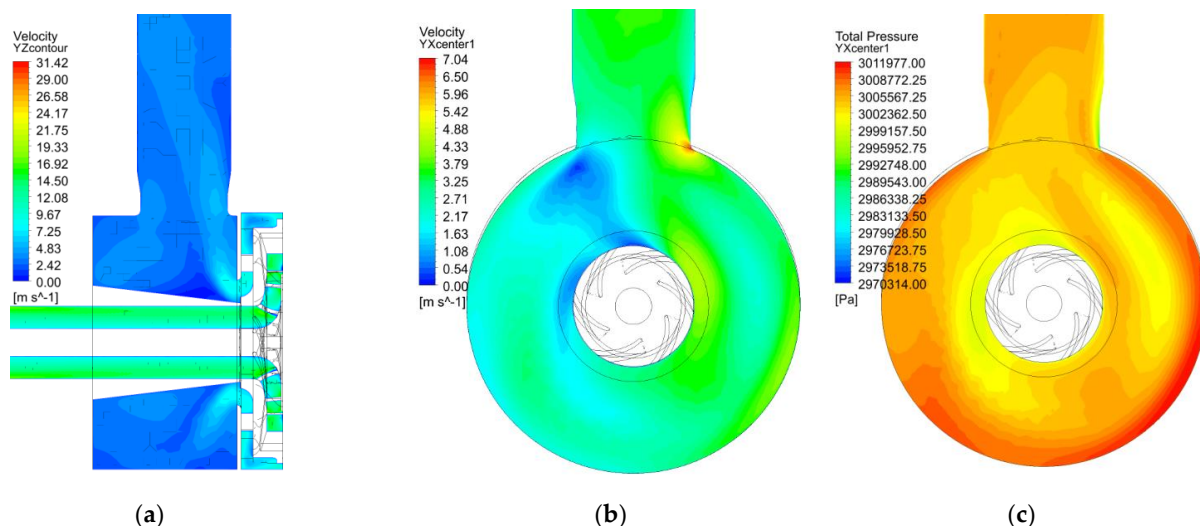


Figure 6. Qualitative picture of the distribution of relative velocity in the ring chamber (a) and in the pressure nozzle of the outlet device (b); pressure in the ring chamber and the discharge nozzle of outlet device (c).

The speed distribution is relatively uniform (Figure 6a). The only zone of reduced velocity (Figure 6b) is explained by the change in the direction of the flow near the outlet tongue. The pressure distribution in the ring chamber and pressure nozzle (Figure 6c) is uniform, with a gradual increase in its value in the direction of movement of the operating fluid from the center to the periphery. A decrease explains this in the dynamic component of the pressure and an increase in its static component. In general, the pressure distribution

is uniform, with no pronounced zones of reduced (blue color) or increased pressure (red color) in the considered pump channels [28].

According to the received data, maximum efficiency is achieved at a flow rate of about 500 m³/h and is 0.74 (Table 2). It is approximately 12–13% higher than for the analog TX 800/70/8-K-2E.

Table 2. Results of parametric tests for the developed pump ACNA 600-35 (fluid density $\rho = 997 \text{ kg/m}^3$; rotation speed $n = 1500 \text{ rpm}$).

Best Efficiency Point (BEP)	Flow Rate	Mass Flow Rate	Pressure Head	Energy Efficiency	Power Consumption
	m ³ /h	kg/s	m	%	kW
0.05	30	8.31	49.91	14	27.2
0.10	60	16.62	47.21	24	28.4
0.20	120	33.23	45.14	40	33.7
0.40	240	66.47	46.85	58	47.3
0.60	360	99.70	47.78	69	63.8
0.80	480	132.93	45.32	74	75.6
1.00	600	166.17	38.44	70	85.3
1.20	720	199.40	27.64	56	90.8
1.40	840	232.63	12.95	30	93.2

The calculations of the axial and radial forces acting on the rotor of the pumping unit ACNA 600-35 are given in Table 3.

Table 3. Calculation of axial and radial forces acting on the rotor of the developed pump ACNA 600-35 (fluid density $\rho = 997 \text{ kg/m}^3$; rotation speed $n = 1500 \text{ rpm}$).

Best Efficiency Point (BEP)	Flow Rate	Mass Flow Rate	Pressure Head	Axial Force
	m ³ /h	kg/s	m	kN
0.05	30	8.31	49.9	7426
0.10	60	16.62	47.2	7266
0.20	120	33.23	45.1	7408
0.40	240	66.47	46.9	8630
0.60	360	99.70	47.8	9696
0.80	480	132.93	45.3	9941
1.00	600	166.17	38.4	8876
1.20	720	199.40	27.6	6352
1.40	840	232.63	13.0	2117

3.2. Strength and Vibration Reliability of the Pump’s Elements

Numerical modeling of the shaft has resulted in different oscillation frequencies and corresponding mode shapes (Figure 7).

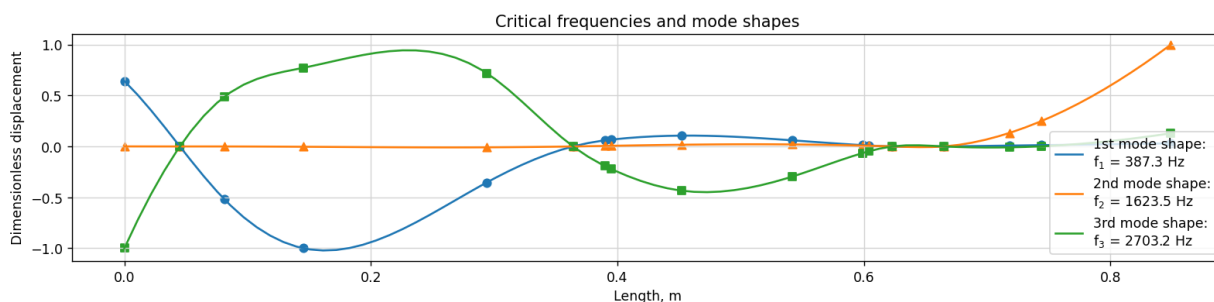
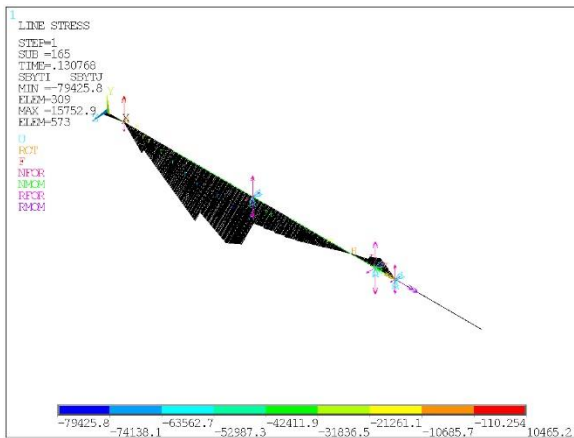


Figure 7. Eigenfrequencies and mode shapes.

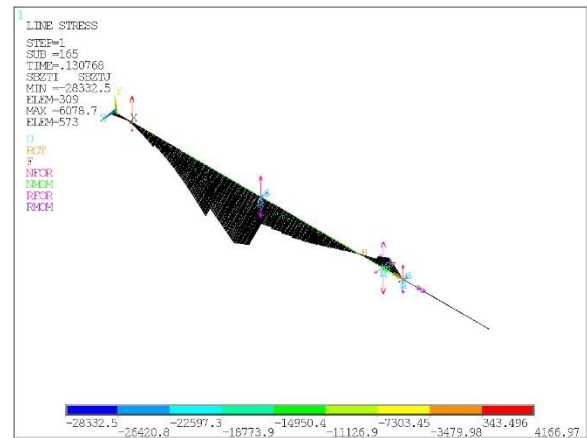
A cyclically, time-varying, forcing load generates a cyclically variable response of the model. Using the ANSYS CFX 19 software, the calculation of purely forced vibrations of the shaft under the action of the centrifugal force generated by imbalance of the impeller was carried out.

The frequency of the exciting force is much lower than the first frequency (24.75 Hz \ll 387.3 Hz). Therefore, the rotor is rigid. Permissible unbalance is defined according to ISO 1940-1:2003 for balancing accuracy class G2.5. The magnitude of the excitation force is $n = 1485$ rpm (24.75 Hz).

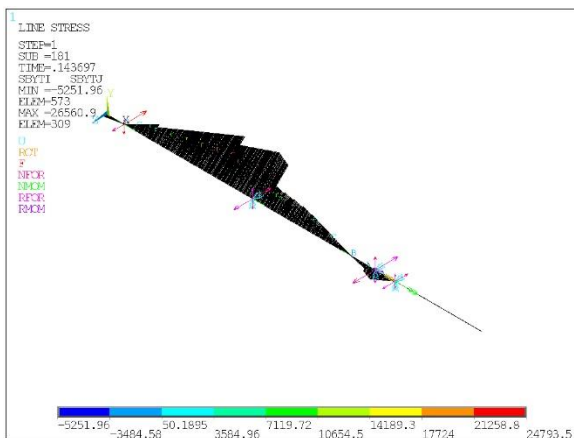
Since the frequency of the excited force is lower than the first natural frequency of oscillations, resonance is not achieved in the ANSYS APDL 19.0 software complex, despite Harmonic, a more complex study of dynamic transient processes, being carried out for the calculation scheme of the shaft additionally loaded in the center of the impeller's mass by harmonic centrifugal force with projections $F_{z_{reg}} = F_{reg} \cos(\Omega t)$ and $F_{y_{reg}} = F_{reg} \sin(\Omega t)$. To preserve the calculation model's static determinability and assume the absence of accompanying torsional vibrations of the shaft, the proper support is fixed from rotation relative to the shaft axis [29]. The time of the establishment of the oscillations of four complete revolutions is investigated: $t_{fin} = 4 \cdot (60/n)$. The results are shown in Figure 8.



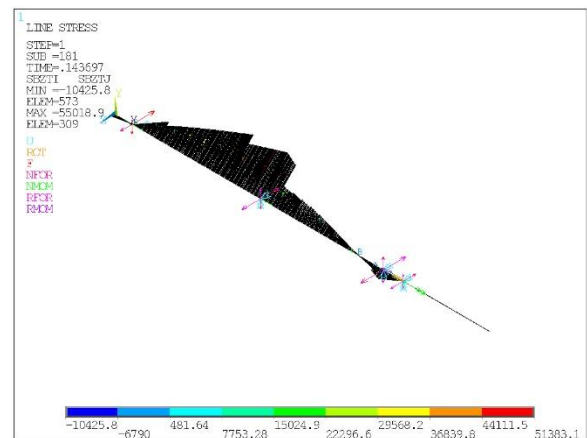
(a)



(b)



(c)



(d)

Figure 8. Cont.

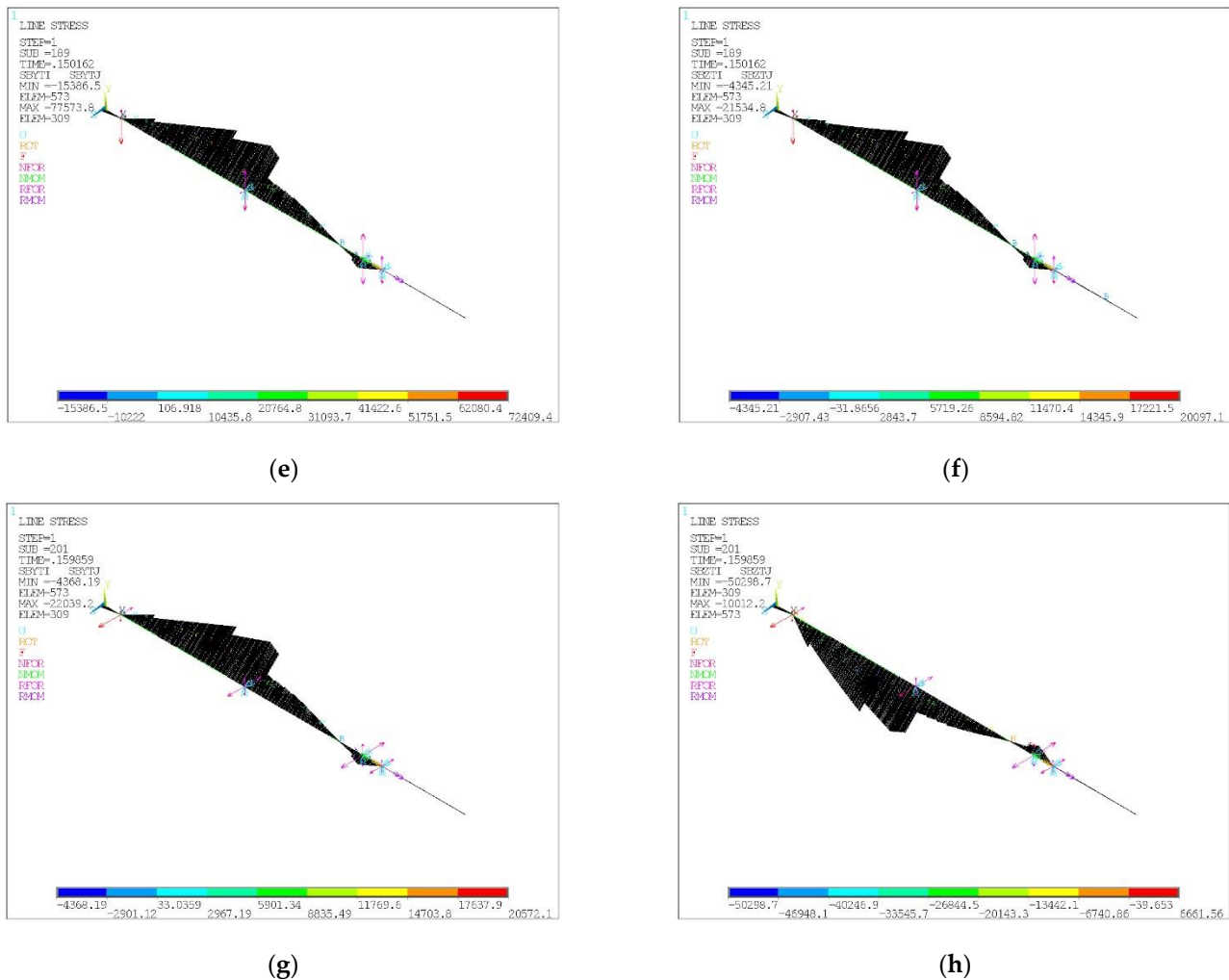


Figure 8. Plots of maximum normal stresses σ_{My} and σ_{Mz} (Pa), from bending moments M_y and M_z , respectively: (a) σ_{My} at 131 ms; (b) σ_{Mz} at 131 ms; (c) σ_{My} at 144 ms; (d) σ_{Mz} at 144 ms; (e) σ_{My} at 150 ms; (f) σ_{Mz} at 150 ms; (g) σ_{My} at 160 ms; (h) σ_{Mz} at 160 ms.

As it can be seen, the maximum stresses almost always occur in the hinged support formed by the spherical roller bearing.

4. Discussion

According to the results of parametric tests (Table 2) using the ANSYS CFX 19.0 software [30,31], conclusions can be made about the nature of the pressure and energy characteristics of the developed unit of the pumping unit ACNA 600-35.

Analysis of the qualitative picture of the distribution of relative speed in the impeller intervane channels (Figure 4) proves the high quality of the design of its flowing part. Particularly, the distribution of pressure in the impeller's intervane channels corresponding with the research [27,32] proves the correctness of the selection of the number of blades (Figure 4a).

The study was carried out for Q modes from 30 to 840 m³/h, which corresponds with the flow rate from 0.05 to 1.40 of the best efficiency point (BEP) Q_{BEP} .

The installation angle of the impeller blade corresponds to the angle of flow, as evidenced by the qualitative picture of relative velocity distribution at the inlet of the impeller. The presence of an insignificant zone of slightly increased speed (red color near the leading edge) indicates the presence of an insignificant angle of attack, which is designed to achieve the required pressure value with high energy efficiency. A small zone of reduced relative velocity is observed in the impeller's intervane channels in the impeller's outlet direction

from the blade's rear side. This happens due to the slight diffusivity of the impeller's interblade channel in the direction from the inlet to the outlet of the impeller. Since this area is relatively small, we can assert the high quality of the design of the impeller's interblade channels, which does not lead to significant hydraulic losses. The distribution of relative speed over the entire surface of the operating side of the blade is uniform. It does not contain substantial zones of increase or decrease of this parameter, which indicates the high quality of the design of the blade and the smoothness of the flow of the operating fluid onto it without significant zones of hydraulic losses.

Thus, the developed pumping unit ACNA 600-35 unit is characterized by increased energy efficiency compared with existing analogs [33].

The valuable practical significance of the research is in regards to the need to modernize pumps for cooling systems of the holding pool and the industrial circuit at Zaporizhska, Rivne, South Ukrainian, and Khmelnytsky NPPs to overcome today's challenges concerning emergencies at Ukrainian NPPs.

The head in the best efficiency point $Q_{BEP} = 600 \text{ m}^3/\text{h}$ is 38.5 m, which is 3.5 m or 10% higher than that of the analog pump TX 800/70/8-K-2E.

The operating zone of the pump, which is characterized by a decrease in efficiency of the pump by no more than 5% compared with the value at the BEP, lies within the flow rate $Q = (0.6\text{--}1.1) \cdot Q_{BEP}$, or $Q = 360\text{--}660 \text{ m}^3/\text{h}$, which provides a wide range of pump operation with high energy efficiency. The power consumed by the pump in the operating range lies within $N = 63\text{--}81 \text{ kW}$, which allows for the operation of a pumping unit with electric motors with a power of 75–110 kW.

The nature of the pump head characteristic is gently falling, allowing for pump operation even at operating modes $Q = (0.05\text{--}0.50) \cdot Q_{BEP}$ without surging.

It is worth noting that the calculated value of the radial force acting on the pump rotor for all operating modes is insignificant since the developed structural scheme of the flowing part ensures an axisymmetric flow of liquid in the outlet device due to the presence of a non-unit channel in the pump's guide vanes device. In particular, the axial force acting on the rotor of the developed pump ranges from 2.1 kN to 9.9 kN, and $Q = 600 \text{ m}^3/\text{h}$ is 8.9 kN in BEP mode.

The parametric tests for the developed pump prototype will be carried out further by using the facilities of Sumy Machine-Building Cluster of Energy Equipment, particularly at the Interdisciplinary Research Laboratory of Hydrodynamic Pumps and Drives, specialized in experimental research on hydrodynamic machines, development of advanced technologies for the pumping industry, and conducting parametric tests of the flow parts of pumping equipment.

5. Conclusions

Based on the obtained results, the centrifugal pump ACNA 600-35 was developed, which is intended to increase the energy efficiency of the pumping equipment of the holding pool and industrial circuit of the nuclear reactor WWER-1000 of Ukrainian NPPs.

According to the results of the numerical research of hydrodynamic processes in the developed pump flowing part, it was proven that the energy efficiency of the developed pump increased up to 0.74 while operating at BEP mode, which is 0.12–0.13 higher than the indicators of existing analog pumps that operate in these systems.

According to the results of the numerical research on the strength and vibration resistance of the parts and elements of the pump and the pump unit, it was determined that the frequency of the exciting force is much lower than that of the first natural frequency ($24.75 \text{ Hz} \ll 387.3 \text{ Hz}$). The rotor is rigid. Permissible unbalance is defined according to ISO 1940-1:2003 for balancing accuracy class G 2.5. The magnitude of the excitation force is $n = 1485 \text{ rpm}$ (24.75 Hz).

The main advantages of the study are as follows:

- (1) the development of a new, more efficient pump for the needs of the storage pools and cooling systems of the WWER-1000 reactors of NPPs, which will increase their safety levels;

- (2) development of a new type of pump with increased energy efficiency indicators of up to 12% that reduces operation costs when compared with that of the analogs.

The results of the research allow us to significantly reduce (up to 15–20%) the life cycle cost of the developed ACNA 600-35 pump compared with the analog TX 800/70/8-K-2E used in the holding pool and industrial circuit of the WWER-1000 reactors at NPPs.

Thus, the indicated research results can be applied to reduce the energy intensity of the operating processes of NPPs by reducing the energy consumed by the developed pumps.

Additionally, the research results are an essential factor in increasing the reliability and safety of NPPs because of the need to ensure the energy efficiency of pumps for these systems. Overall, the results make it possible to comprehensively increase the degree of energy independence in Eastern Europe.

Author Contributions: Conceptualization, I.P. and V.K.; methodology, V.K.; software, I.P. and O.C.; validation, O.R., O.C. and O.I.; formal analysis, E.K., O.K. and V.I.; investigation, V.K.; resources, O.K. and O.R.; data curation, O.R. and V.I.; writing—original draft preparation, I.P. and V.K.; writing—review and editing, O.I. and E.K.; visualization O.K., O.I., E.K. and V.I.; supervision, I.P.; project administration, I.P. and O.C.; funding acquisition, O.C. All authors have read and agreed to the published version of the manuscript.

Funding: The research was funded by the Ministry of Science and Higher Education of Poland within the projects of Poznan University of Technology “Research in the field of innovative manufacturing techniques, measurement, construction of modern machines and devices and their control,” grant number 0614/SBAD/1565.

Data Availability Statement: The data presented in this study are available on request from the corresponding author.

Acknowledgments: The research was realized within the Ulam NAWA Programme “Application of artificial intelligence system for diagnostics and predictive maintenance of rotary machines,” ordered by the Polish National Agency for Academic Exchange (grant number BPN/ULM/2022/1/00042). Additionally, we appreciate the support of the International Association for Technological Development and Innovations (IATDI) while conducting the research.

Conflicts of Interest: The authors declare no conflict of interest.

Nomenclature

NPP	nuclear power plants
BEP	best efficiency point
WWER-1000	water-water energetic reactor with a capacity of 1000 MW
TX 800/70/8-K-2E	centrifugal chemical pump with the following parameters: flow rate—800 m ³ /h; pressure head—70 m; 8—conventional notation of rotation frequency (960 rpm); K-2E—conventional notation of materials of flowing part elements
ACNA 600-35	centrifugal pump aggregate for the nuclear industry with the following parameters: flow rate—600 m ³ /h; pressure head—35 m
Symbols and Units	
x_i, x_j	coordinate axes (m)
U_i, U_j	velocity components (m/s)
p	pressure (Pa)
t	time (s)
f_i	i -th mass force (N)
$\vec{\omega}$	the angular velocity vector (rad/s)
\vec{r}	the radius vector (m)
\bar{U}_i, \bar{U}_j	time-averaged velocity values (m/s)
\bar{U}'_i, \bar{U}'_j	pulsating components of velocities (m/s)

References

1. Popov, O.; Iatsyshyn, A.; Sokolov, D.; Dement, M.; Neklonskyi, I.; Yelizarov, A. Application of virtual and augmented reality at nuclear power plants. In *Systems, Decision and Control in Energy II*; Springer: Berlin/Heidelberg, Germany, 2021; Volume 346, pp. 243–260. [\[CrossRef\]](#)
2. Fausing Olesen, J.; Shaker, H.R. Predictive maintenance for pump systems and thermal power plants: State-of-the-art review, trends and challenges. *Sensors* **2020**, *20*, 2425. [\[CrossRef\]](#)
3. Popov, O.; Iatsyshyn, A.; Molitor, N.; Iatsyshyn, A.; Romanenko, Y.; Deinega, I.; Mnayarji, G. Human factor in emergency occurrence at NPP during the pandemic COVID-19: New potential risks and recommendations to minimize them. *E3S Web Conf.* **2021**, *280*, 09013. [\[CrossRef\]](#)
4. Mohsen, M.Y.; Soliman, A.Y.; Abdel-Rahman, M.A. Thermal-hydraulic and solid mechanics safety analysis for VVER-1000 reactor using analytical and CFD approaches. *Prog. Nucl. Energy* **2020**, *130*, 103568. [\[CrossRef\]](#)
5. Kumar, A.; Pant, S.; Ram, M. Gray wolf optimizer approach to the reliability-cost optimization of residual heat removal system of a nuclear power plant safety system. *Qual. Reliab. Eng. Int.* **2019**, *35*, 2228–2239. [\[CrossRef\]](#)
6. Miglierini, B.; Kozlowski, T.; Kopecek, V. Uncertainty analysis of rod ejection accident in VVER-1000 reactor. *Ann. Nucl. Energy* **2019**, *132*, 628–635. [\[CrossRef\]](#)
7. Kumar, P.; Singh, L.K.; Kumar, C. An optimized technique for reliability analysis of safety-critical systems: A case study of nuclear power plant. *Qual. Reliab. Eng. Int.* **2018**, *35*, 461–469. [\[CrossRef\]](#)
8. Kovaliov, I.; Ratushnyi, A.; Dzafarov, T.; Mandryka, A.; Ignatiev, A. Predictive vision of development paths of pump technical systems. *J. Phys. Conf. Ser.* **2021**, *1741*, 012002. [\[CrossRef\]](#)
9. Antonenko, S.; Sapozhnikov, S.; Kondus, V.; Chernobrova, A.; Mandryka, A. Creation a universal technique of predicting performance curves for small-sized centrifugal stages of well oil pump units. *J. Phys. Conf. Ser.* **2021**, *1741*, 012011. [\[CrossRef\]](#)
10. Puzik, R.V.; Kovaliov, I.O.; Ratushnyi, O.V.; Dzafarov, T.V.; Petrenko, S.S. The ways to increase the efficiency of the stage of low specific speed. *J. Phys. Conf. Ser.* **2021**, *1741*, 012013. [\[CrossRef\]](#)
11. Kondus, V.; Gusak, O.; Yevtushenko, J. Investigation of the operating process of a high-pressure centrifugal pump with taking into account of improvement the process of fluid flowing in its flowing part. *J. Phys. Conf. Ser.* **2021**, *1741*, 012012. [\[CrossRef\]](#)
12. Capurso, T.; Bergamini, L.; Torresi, M. Design and CFD performance analysis of a novel impeller for double suction centrifugal pumps. *Nucl. Eng. Des.* **2019**, *341*, 155–166. [\[CrossRef\]](#)
13. Zhang, F.; Yuan, S.; Fu, Q.; Pei, J.; Chen, J. Transient flow characteristics during variable operating conditions of the centrifugal charging pump in 1000 MW nuclear power plant. *Proc. Inst. Mech. Eng. Part E J. Process Mech. Eng.* **2015**, *229*, 233–242. [\[CrossRef\]](#)
14. Zhou, F.M.; Wang, X.F. The effects of blade stacking lean angle to 1400 MW canned nuclear coolant pump hydraulic performance. *Nucl. Eng. Des.* **2017**, *325*, 232–244. [\[CrossRef\]](#)
15. Tao, R.; Xiao, R.; Liu, W. Investigation of the flow characteristics in a main nuclear power plant pump with eccentric impeller. *Nucl. Eng. Des.* **2018**, *327*, 70–81. [\[CrossRef\]](#)
16. Song, Y.; Xu, R.; Yin, J.; Wang, D.; Xia, S. Experimental study on the effect of non-uniform flow on the vibration characteristics of the reactor coolant pump. In Proceedings of the International Conference on Nuclear Engineering, ICONE, Tsukuba, Japan, 19–24 May 2019; p. 150404.
17. Shi, Q.; Ye, P.; Zhao, G. Design of a two-stage centrifugal pump for nuclear systems. In Proceedings of the International Conference on Nuclear Engineering, ICONE, Charlotte, NC, USA, 26–30 June 2016; Volume 5, p. 124474. [\[CrossRef\]](#)
18. Liu, Z.; Luo, N.; Ai, Q. Research on fault pattern recognition model of nuclear power plant water pump based on frequency-domain data attention mechanism. *Nucl. Power Eng.* **2021**, *42*, 203–208. [\[CrossRef\]](#)
19. Jiao, Z.; Cai, L.; Zhang, L.; Hu, L.; Liu, X. Model for calculating idling of nuclear power coolant pump considering coolant kinetic energy in pipeline. *Nucl. Power Eng.* **2022**, *43*, 48–51. [\[CrossRef\]](#)
20. Kondus, V.Y.; Kottenko, A.I. Investigation of the impact of the geometric dimensions of the impeller on the torque flow pump characteristics. *East.-Eur. J. Enterp. Technol.* **2017**, *4*, 25–31. [\[CrossRef\]](#)
21. Ratushnyi, A.V.; Sokhan, A.O.; Kovaliov, I.O.; Mandryka, A.S.; Ignatiev, A.S. Modernization of centrifugal impeller blades. *J. Phys. Conf. Ser.* **2021**, *1741*, 012009. [\[CrossRef\]](#)
22. Kondus, V.Y.; Kalinichenko, P.V.; Gusak, O.G. A method of designing of torque-flow pump impeller with curvilinear blade profile. *East.-Eur. J. Enterp. Technol.* **2018**, *3*, 29–35. [\[CrossRef\]](#)
23. Kondus, V.; Puzik, R.; German, V.; Panchenko, V.; Yakhnenko, S. Improving the efficiency of the operating process of high specific speed torque-flow pumps by upgrading the flowing part design. *J. Phys. Conf. Ser.* **2021**, *1741*, 012023. [\[CrossRef\]](#)
24. Syomin, D.; Rogovyi, A. Features of a working process and characteristics of irrotational centrifugal pumps. *Procedia Eng.* **2020**, *39*, 231–237. [\[CrossRef\]](#)
25. Cheng, K.; Wang, C.; Fang, Y.; Wang, J. Calculation and analysis of stable operation of feed water pumps for floating nuclear power stations under marine conditions. *J. Phys. Conf. Ser.* **2020**, *1600*, 012077. [\[CrossRef\]](#)
26. Rogovyi, A.; Khovansky, S.; Grechka, I.; Pitel, J. The wall erosion in a vortex chamber supercharger due to pumping abrasive mediums. In *Design, Simulation, Manufacturing II: The Innovation Exchange*; Lecture Notes in Mechanical Engineering; Springer: Cham, Switzerland, 2019; pp. 682–691. [\[CrossRef\]](#)
27. Kostornoi, A.S.; Tkach, P.Y.; Bondariev, O.O.; Podopryhora, N.N. Design of impeller blades in the intermediate stage of centrifugal pump to a preset shape of meridional flow pattern. *J. Phys. Conf. Ser.* **2021**, *1741*, 012005. [\[CrossRef\]](#)

28. Fang, Y.; Liu, X.; Luo, X.; Qiao, L.; Wang, C.; Sun, H. Study on the configuration of feed water pump for floating nuclear power plant. *AIP Conf. Proc.* **2019**, *2154*, 020031. [[CrossRef](#)]
29. Panchenko, A.; Voloshina, A.; Titova, O.; Panchenko, I. The influence of the design parameters of the rotors of the planetary hydraulic motor on the change in the output characteristics of the mechatronic system. *J. Phys. Conf. Ser.* **2021**, *1741*, 012027. [[CrossRef](#)]
30. Chernobrova, A.; Sotnik, M.; Moloshnyi, O.; Antonenko, S.; Boiko, V. Influence of different volute casings theoretical methods design on pump working processes. *J. Phys. Conf. Ser.* **2021**, *1741*, 012014. [[CrossRef](#)]
31. Huang, S.; Song, Y.; Yin, J.; Xu, R.; Wang, D. Research on pressure pulsation characteristics of a reactor coolant pump in hump region. *Ann. Nucl. Energy* **2022**, *178*, 109325. [[CrossRef](#)]
32. Mandryka, A.; Majid, A.P.; Ratushnyi, O.; Kulikov, O.; Sukhostavets, D. Ways for improvement of reverse axial pumps. *J. Eng. Sci.* **2022**, *9*, D14–D19. [[CrossRef](#)]
33. Sotnyk, M.I.; Moskalenko, V.V.; Strokin, O.O.; Antonenko, S.S.; Sapozhnikov, S.V. Influence of construction and operating pump parameters on pressure pulsations amplitude. *J. Phys. Conf. Ser.* **2021**, *1741*, 012010. [[CrossRef](#)]

Disclaimer/Publisher’s Note: The statements, opinions and data contained in all publications are solely those of the individual author(s) and contributor(s) and not of MDPI and/or the editor(s). MDPI and/or the editor(s) disclaim responsibility for any injury to people or property resulting from any ideas, methods, instructions or products referred to in the content.